Volume 23, No 4 | International Journal of Radiation Research, October 2025

Cyclotron 30 MeV 1.5 mA shielding design for boron neutron capture therapy

A.R.W. Wicaksana[1], A. Muharini[1], Y. Sardjono[2], G.S. Wijaya[2], Z. Ismail[2,3], I.M. Triatmoko[2], S. Ulya[2*], H. Prasetio[2], N. Nuraeni[2], N.R. Hidayati[2], Fendinugroho[2], Y. Kasesaz[4]

[1]Department of Nuclear Engineering and Engineering Physics, Faculty of Engineering, Universitas Gadjah Mada, 2 Grafika Street, Yogyakarta 55281, Indonesia
[2]Research Center for Safety, Metrology, and Nuclear Quality Technology, Research Organization for Nuclear Energy, National Research and Innovation Agency Indonesia
[3]Department of Physics, Faculty of Mathematics and Natural Sciences, Sekip Utara BLS 21 Yogyakarta 55281, Indonesia
[4]Nuclear Science and Technology Research Institute (NSTRI), Tehran, Iran

► ***Original article***

***Corresponding author:**
Syarifatul Ulya, Ph.D,
***E-mail:** syar015@brin.go.id*

Received: May 2024
Final revised: April 2025
Accepted: May 2025

Int. J. Radiat. Res., October 2025; 23(4): 935-943

DOI: 10.61186/ijrr.23.4.15

Keywords: *BNCT, radiation shielding, Monte Carlo simulation, PHITS, concrete materials.*

ABSTRACT

Background: Effective radiation shielding in Boron Neutron Capture Therapy (BNCT) facilities is essential to protect patients, staff, and the environment from secondary radiation. This study aims to determine the optimal thickness of Portland, boron, and barite concretes for shielding the Beam Shaping Assembly (BSA) in BNCT facilities, ensuring compliance with International Atomic Energy Agency (IAEA) and Indonesia's BAPETEN (Nuclear Energy Regulatory Agency of Indonesia) safety standards. ***Materials and Methods:*** Monte Carlo simulations were performed using the Particle and Heavy Ion Transport Code System (PHITS) to model radiation interactions. The shielding performance of the three concretes was evaluated across five critical areas of the BSA: front, left side, external labyrinth, top, and bottom, utilizing 100,000,000 particles for statistical accuracy. ***Results:*** Barite concrete required the least thickness due to its high density and superior photon attenuation, with optimal thicknesses of 0.56 m, 0.4 m, 1.0 m, 0.4 m, and 0.32 m in the respective areas. Boron concrete provided enhanced neutron protection with thicknesses of 0.79 m, 0.35 m, 1.0 m, 0.45 m, and 0.32 m. Portland concrete, while needing greater thickness for gamma shielding, remained cost-effective and accessible with thicknesses of 0.7 m, 0.5 m, 1.0 m, 0.5 m, and 0.37 m. ***Conclusion:*** All three concretes met IAEA and BAPETEN safety standards. Barite concrete was most effective for photon attenuation, boron concrete excelled in neutron protection, and Portland concrete offered a practical balance between effectiveness and cost. These findings aid in designing safe and efficient BNCT facilities, especially in resource-limited settings.

INTRODUCTION

Cancer continues to be a global health concern, with 19.3 million new cases and almost 10 million fatalities documented worldwide in 2020 [1-3]. Asia, representing over fifty percent of the overall cases, includes Indonesia, which reported 396,914 cancer diagnoses, accounting for 2.05% of the global total [4-6]. This burden is exacerbated by ageing populations, lifestyle factors including tobacco and alcohol consumption, and disparities in healthcare access, especially in low- and middle-income countries (LMICs) in Southeast Asia [1, 5, 7-9]. The rising prevalence of cancer in older adults, who represented 64% of new cases in 2020 and are expected to increase through 2040, alongside the prevalence of modifiable risk factors such as elevated body mass index and poor dietary practices, complicates this issue [7, 10, 11]. Notwithstanding progress in cancer treatment, access to contemporary therapies is still constrained in numerous LMICs, underscoring the necessity for innovative approaches, including enhanced screening initiatives, risk factor mitigation, and equitable health service access to alleviate the global cancer burden [12, 13].

BNCT has emerged as a promising cancer therapy tool in the quest for more effective alternatives. BNCT specifically targets and eradicates tumour cells while preserving healthy tissue via a nuclear reaction between boron-10 isotopes and low-energy neutrons, generating particles with high linear energy transfer (LET) that effectively eliminate tumour cells [14-16]. Recent advancements in BNCT, encompassing the creation of more targeted boron delivery agents and accelerator-based neutron source technologies, have broadened its applicability to intricate malignancies such as glioblastoma multiforme and head and neck cancers, exhibiting survival advantages compared to

[DOI: 10.61186/ijrr.23.4.15]

traditional therapies [17-19]. The incorporation of BNCT with personalised medicine strategies, including functional imaging and proteomics, has highlighted its efficacy as a precision therapy customised to specific tumour profiles [20]. Nonetheless, obstacles persist in enhancing boron administration and neutron source technologies to optimise therapeutic effectiveness while reducing toxicity [20, 21].

A critical challenge in the implementation of BNCT is the assurance of safety via effective radiation shielding design. BNCT generates gamma radiation, thermal neutrons, and fast neutrons, which present hazards to patients, medical personnel, and the general populace [19-23]. Regulatory entities, like the IAEA and BAPETEN, have established yearly exposure thresholds of 20 mSv for personnel and 1 mSv for the general populace, adhering to the ALARA (As Low As Reasonably Achievable) principle [24, 25]. Effective shielding design utilising materials such barite concrete, paraffin, and polyethylene borate is crucial for adherence to these radiation limitations [26, 27]. Monte Carlo simulations are indispensable in the design and optimisation of radiation shielding, facilitating precise predictions of radiation interactions and the refinement of shielding material compositions for diverse medical applications [28, 29]. The advancement of sophisticated shielding materials and computational techniques has enhanced the safety and efficacy of BNCT, guaranteeing secure and effective treatment for patients [30, 31].

This study offers a comparative investigation of three prevalent shielding materials-Portland concrete, boron concrete, and barite concrete-regarding their efficacy in attenuating radiation emissions in BNCT facilities. This study employs Monte Carlo simulations through PHITS to thoroughly evaluate the dose reduction effectiveness of multiple materials across varied BSA configurations, in contrast to prior research that concentrated on a singular material or standard shielding design. This study's novelty is rooted in its emphasis on feasibility and cost-efficiency, particularly within a resource-constrained environment like Indonesia. This study presents a customised strategy for the safe application of BNCT in emerging regions by integrating regulatory compliance with modern simulation methodologies. The results underscore the viability of boron concrete and barite concrete as substitutes for conventional Portland concrete, effectively resolving performance and logistical challenges in radiation shielding design.

MATERIALS AND METHODS

Simulation framework

The study utilized the Particle and Heavy Ion Transport Code System (PHITS) developed by the Japan Atomic Energy Agency as the principal simulation instrument. PHITS was employed to precisely simulate and determine the optimal wall thickness necessary for radiation shielding in BNCT facilities. This study's simulations examined three different types of concrete materials: Portland concrete, barite concrete, and boron concrete. The materials were chosen based on their availability, cost-effectiveness, and efficacy in attenuating various forms of radiation. The study sought to determine the ideal composition and thickness of these materials by modeling their shielding performance to comply with safety criteria [32].

Materials selection

Portland concrete was chosen as a construction-grade material readily accessible in Indonesia, it adheres to SNI (Indonesian National Standard) and international requirements. Portland concrete is commonly utilized in building applications, valued for its availability and compliance with safety standards in shielding design.

Boron concrete was selected for its excellent neutron absorption properties, due to its boron content. Boron substantially improves the material's ability to attenuate fast neutrons, rendering it suitable for crucial components of the BSA.

This study also evaluated barite concrete for its high density and excellent photon attenuation characteristics. The high density of barite renders it especially effective in attenuating gamma radiation, hence enhancing the overall protective efficacy of the shielding system.

Boron stainless steel was employed for door shielding due to its neutron absorption capabilities. Boron stainless steel is acknowledged for its industrial-grade shielding properties, offering essential protection in environments where neutron penetration presents considerable hazards.

The specific compositions of the materials utilized in this study are delineated in table 1. The table presents the atomic percentage and density for each material, including Portland concrete, boron concrete, barite concrete, and boron stainless steel.

Geometry and configuration

The BSA consists of a 39 cm-thick aluminum moderator, an 8.2 cm-thick lithium fluoride (LiF_2) fast neutron filter, and a 0.5 cm-thick boron carbide (B_4C) thermal neutron filter. Gamma reflectors composed of PbF_2, Pb, and Bi are strategically arranged to enhance neutron flux directed at the target. The dimensions and configurations are derived from the research of Ardana et al., establishing a basis for incorporating shielding designs that reduce secondary radiation. The BSA modeling used is shown in figure 1 [33].

[DOI: 10.61186/ijrr.23.4.15]

Table 1. Atomic composition and density of shielding materials. This table lists the atomic fractions of elements in Portland Concrete, Boron Concrete, Barite Concrete, and Boron Stainless Steel, along with their densities (kg/m³), to evaluate their radiation attenuation properties for BNCT facilities [32].

Element	Atomic Fraction			
	Portland Concrete	Boron Concrete	Barite Concrete	Boron Stainless Steel
H	0.168759	0.147522	0.109602	-
C	0.001416	-	-	0.00174
O	0.562524	0.560939	0.600189	-
Na	0.011838	0.013975	-	-
Mg	0.0014	0.002513	0.001515	-
Al	0.021354	0.006298	0.004777	0.009304
Si	0.204115	0.031293	0.011473	-
K	0.005656	0.000679	-	-
Ca	0.018674	0.041474	0.038593	-
Fe	0.004264	0.010413	0.026213	-
B	-	0.025543	-	0.048827
F	-	-	-	-
S	-	0.075769	0.103654	0.000244
Zn	-	0.002679	-	-
Ba	-	0.077592	0.103983	-
Cr	-	-	-	0.19096
Mn	-	0.000097	-	0.009512
Ni	-	-	-	0.082359
P	-	-	-	0.000388
Density	2300 kg/m^3	3100 kg/m^3	3350 kg/m^3	7870 kg/m^3

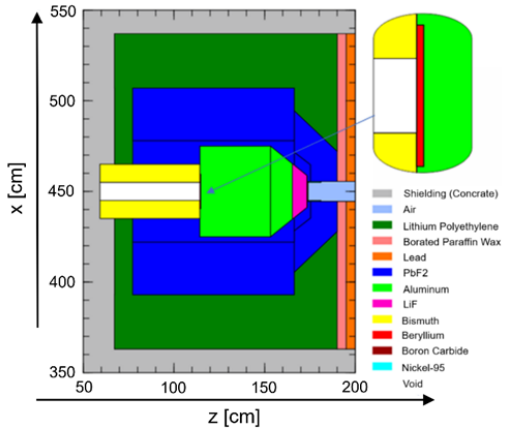

Figure 1. Top view of the BSA geometry used in the Monte Carlo simulations for BNCT shielding design with the component shielding (concreate), air, lithium polyethylen, borated paraffin wax, lead, PbF2, almunium, LiF, bismuth, beryllium, boron carbide, nickel-95 void.

The simulation room has defined dimensions of 3 meters in length, width, and height. Wall thickness variations are concentrated in three primary areas: the front of the BSA, the left side of the BSA, and the labyrinth. The thickness of each section is meticulously designed according to the material's ability to attenuate gamma and neutron radiation generated during operation, as demonstrated in figures 2 and 3. To prevent radiation leakage beyond the room, the labyrinth features a combination of shielding walls and doors constructed from boron stainless steel.

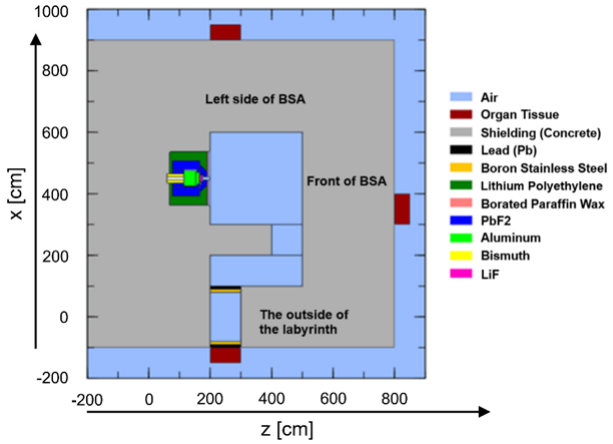

Figure 2. Top view of the simulation room used for BNCT shielding design. The room dimensions are 3 meters in length, width, and height, with designated areas for Front BSA, Left BSA, Outside Labyrinth, Upper Wall, and Lower Wall shielding sections.

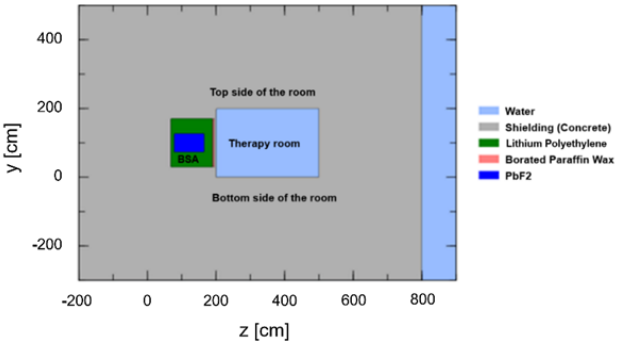

Figure 3. Front view of the simulation room layout for BNCT shielding design, providing a vertical perspective of the room's structure from water, shielding (concrete), lithium, borated paraffin wax, PbF2.

RESULTS

Shielding design using portland concrete

As mentioned before, Portland concrete has a lower density compared to other concrete varieties, which directly influences its shielding performance. The lower density results in reduced efficiency of gamma radiation shielding, necessitating a substantial thickness to prevent radiation from escaping the chamber.

The shielding design process commenced with an initial concrete thickness of 3 meters. Through a series of iterative simulations aimed at optimizing the thickness while adhering to safety standards, the thickness was progressively reduced to 2 meters. The final optimized design established a concrete thickness of 0.7 meters for the front of the BSA. Furthermore, the left side wall of the BSA was determined to be 0.5 meters thick, the inner labyrinth required a thickness of 1 meter, and the external labyrinth was optimized to a thickness of 0.2 meters. The top layer of the shielding was finalized at 0.5

[DOI: 10.61186/ijrr.23.4.15]

meters, while the bottom layer was set at 0.37 meters. It was observed that labyrinth optimization reached its practical limits due to the presence of doors, which constrained further thickness reductions.

Figure 4 illustrates the dose distribution achieved with the optimal Portland concrete shielding design. Along the Z-axis, the shielding thickness of 0.7 meters achieved a maximum radiation reduction of 2.2022 × 10^{-2} μSv/h, which is below BAPETEN's safety limit of 0.01 mSv/week.

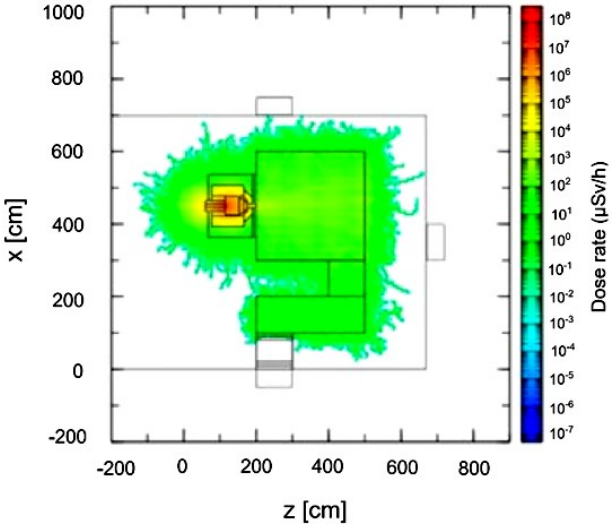

Figure 4. Radiation dose distribution within the BNCT facility using the optimal Portland concrete shielding design.

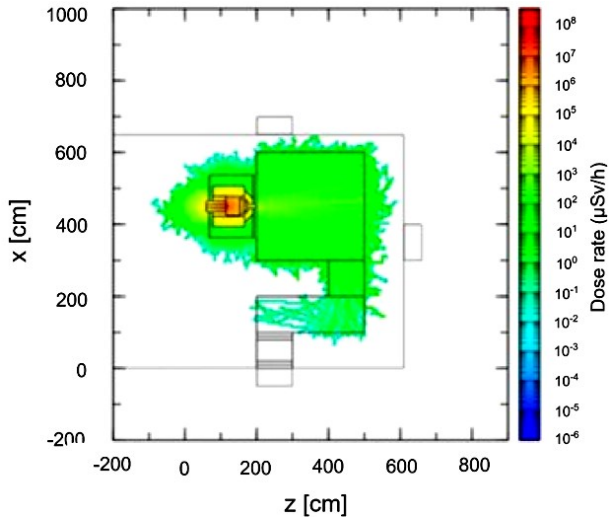

Figure 5. Radiation dose distribution within the BNCT facility utilizing the optimal Boron concrete shielding design.

In the X-axis distribution, the shielding design revealed that the left labyrinth, with a thickness of 0.5 meters, recorded a dose rate of 4.2050 × 10^{-2} μSv/h, and the external labyrinth, at 0.2 meters thick, recorded a rate of 7.7202 × 10^{-2} μSv/h. Both values remained within the permissible safety limits. Similarly, the Y-axis distribution indicated that the top shielding layer of 0.5 meters attenuated radiation to 2.7052 × 10^{-2} μSv/h, and the bottom layer of 0.37 meters reduced it to 7.4808 × 10^{-2} μSv/h, both compliant with regulation standards. The attenuation coefficient for Portland concrete resulted in a value of 3406.54 m^2.

Shielding design using boron concrete

Boron concrete, referred to as Boron Frits-baryte in the compendium, incorporates boron to significantly enhance its neutron attenuation properties. With a density of 3.1 kg/m^3, boron concrete is classified as intermediate among the three types of density fluctuations and excels in absorbing fast neutrons up to a specific thickness. The optimized shielding design using boron concrete featured a thickness of 0.79 meters at the front of the BSA, 0.35 meters for the left labyrinth wall, and 0.1 meters for the outer labyrinth. The top and bottom shielding layers were determined to be 0.45 meters and 0.32 meters thick, respectively. Despite the enhanced attenuation capabilities, the presence of doors in the lower half of the maze limited further optimization of the labyrinth's thickness.

Figure 5 presents the dose distribution for the boron concrete shielding design, confirming its effectiveness in reducing radiation exposure with a reduced thickness compared to Portland concrete. Along the Z-axis, a shielding thickness of 0.79 meters reduces radiation exposure to 8.0175 × 10^{-2} μSv/h, which is well below Indonesia regulation safety limits. In the X-axis distribution, the left labyrinth with a thickness of 0.35 meters achieved a dose rate of 6.3016 × 10^{-2} μSv/h, while the outer labyrinth at 0.1 meters achieved 5.2439 × 10^{-2} μSv/h, both within safe limits.

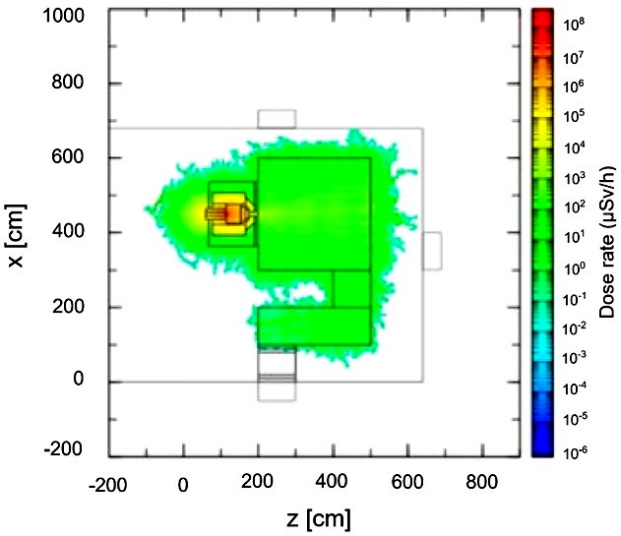

Figure 6. Radiation dose distribution within the BNCT facility employing the optimal Barite concrete shielding design.

The Y-axis distribution indicates that the top shielding layer of 0.45 meters attenuates radiation to 9.1259 × 10^{-2} μSv/h, and the bottom layer of 0.32 meters reduces it to 4.9972 × 10^{-2} μSv/h, both compliant with BAPETEN standards. The attenuation coefficient for boron concrete was calculated to be

[DOI: 10.61186/ijrr.23.4.15]

5844.41 m^2, reflecting its enhanced shielding capability due to the presence of boron.

Shielding design using barite concrete

Barite concrete was selected for its superior density and high atomic number, making it exceptionally effective for photon attenuation. The optimized barite concrete shielding design included a thickness of 0.56 meters at the front of the BSA, 0.4 meters for the left labyrinth wall, and 0.15 meters for the outer labyrinth. The top and bottom shielding layers were finalized at 0.4 meters and 0.32 meters, respectively. Similar to the other designs, the presence of double doors in the labyrinth restricted further thickness optimization.

Figure 6 illustrates the dose distribution for the barite concrete shielding design, confirming its effectiveness in attenuating radiation. Along the Z-axis, a shielding thickness of 0.56 meters reduces radiation intensity to 7.5956 × 10^{-2} µSv/h, which is below BAPETEN's safety threshold. In the X-axis distribution, the left labyrinth with a thickness of 0.4 meters achieved a dose rate of 6.6979 × 10^{-2} µSv/h, while the outer labyrinth at 0.15 meters achieved 8.2309 × 10^{-2} µSv/h, both within permissible limits.

The Y-axis distribution indicates that the top shielding layer of 0.4 meters attenuates radiation to 9.0756 × 10^{-2} µSv/h, and the bottom layer of 0.32 meters reduces it to 9.4850 × 10^{-2} µSv/h, both compliant with regulation standards. Although the exact attenuation coefficient for barite concrete was not explicitly provided, it is inferred to be higher due to its increased density and atomic number.

A comparative analysis of the three concrete types -Portland, Boron, and Barite-revealed distinct differences in both shielding thickness and dose rates across various sections of the BSA. Table 2 summarizes the wall thicknesses required for each material type. Portland concrete required the greatest thickness in most sections, particularly the front (0.7 meters) and inner labyrinth (1 meter), to compensate for its lower density and attenuation coefficient. Boron concrete exhibited intermediate thickness requirements, with slightly increased thickness at the front (0.79 meters) but reduced thickness in other sections due to enhanced neutron attenuation from boron. Barite concrete demonstrated the lowest thickness requirements across most sections, especially the front (0.56 meters), owing to its high density and atomic number, which contribute to superior photon attenuation.

Table 3 compares the dose rates per wall for each material type. Portland concrete showed moderate to high dose rates, particularly in the outer labyrinth (7.7202 × 10^{-2} µSv/h), necessitating thicker walls to maintain safety standards. Boron concrete generally achieved lower dose rates across most sections, with the highest being 9.1259 × 10^{-2} µSv/h in the upper wall, which is within safety limits. Barite concrete, while effective, showed some sections like the outside labyrinth (8.2309 × 10^{-2} µSv/h) approaching the upper safety limits, indicating precise shielding requirements.

Table 2. Optimized Shielding Thickness for Portland, Boron, and Barite Concretes in BNCT BSA Areas. Thicknesses are provided for Front BSA, Left BSA, Outside Labyrinth, Upper Wall, and Lower Wall to ensure compliance with safety standards.

Material Type	Front BSA	Left BSA	Outside Labyrinth	Upper Wall	Lower Wall
Portland Concrete	0.7 m	0.5 m	0.2 m	0.5 m	0.37 m
Boron Concrete	0.79 m	0.35 m	0.1 m	0.45 m	0.32 m
Barite Concrete	0.56 m	0.4 m	0.15 m	0.4 m	0.32 m

Table 3. Radiation Dose Rates (×10^{-2} µSv/h) for Portland, Boron, and Barite Concretes in Various BSA Sections. Dose rates are measured for Front BSA, Left BSA, Outside Labyrinth, Upper Wall, and Lower Wall.

Material Type	Front BSA	Left BSA	Outside Labyrinth	Upper Wall	Lower Wall
Portland Concrete	2.2022	4.2050	7.7202	2.7052	7.4808
Boron Concrete	8.0175	6.3016	5.2439	9.1259	4.9972
Barite Concrete	7.5956	6.6979	8.2309	9.0756	9.4850

The analysis of thickness and dose rates underscores the trade-offs between material properties and practical implementation. While higher density concretes like barite offer superior shielding performance, their increased cost and limited availability may impact their feasibility for widespread use. Conversely, Portland concrete remains a practical option due to its accessibility and compliance with local standards, despite the need for greater thickness to achieve similar protective outcomes.

DISCUSSION

The evaluation of Portland, Boron, and Barite concretes revealed significant variations in their shielding performances against neutron and gamma radiation within the cyclotron chamber's BSA. Each concrete type exhibited unique properties that influenced its attenuation capabilities, thickness requirements, and overall feasibility for implementation.

Portland concrete demonstrated considerable effectiveness in neutron shielding due to its sparse atomic arrangement and the presence of fewer highly energetic atoms. These characteristics facilitate the absorption and attenuation of neutron radiation, making Portland concrete a viable material for

[DOI: 10.61186/ijrr.23.4.15]

environments where neutron shielding is paramount. However, its lower density, as compared to other concrete variants, results in diminished efficiency in gamma radiation shielding. This limitation necessitates a greater thickness of Portland concrete to achieve the desired attenuation levels for gamma rays. The final optimized design required a thickness of 0.7 meters for the front shielding of the BSA, which, while effective, may present practical challenges in terms of space and material costs.

The attenuation coefficient calculated for Portland concrete was 3406.54 m^2. This relatively modest value underscores the necessity for increased thickness to meet safety standards, particularly for gamma radiation. The iterative design process revealed that while Portland concrete is sufficiently effective for neutron attenuation, its performance for gamma shielding is less optimal, thereby requiring compensatory measures such as increased material thickness.

Incorporating boron into concrete significantly enhanced its neutron attenuation capabilities. Boron is renowned for its high neutron cross-section, making boron-infused concrete exceptionally effective in absorbing fast neutrons. The Boron Frits-baryte concrete, with a density of 3.1 kg/m^3, exhibited an attenuation coefficient of 5844.41 m^2, nearly double that of Portland concrete. This substantial improvement allows for a reduction in shielding thickness while maintaining compliance with safety standards.

The optimized design utilizing boron concrete required a front shielding thickness of 0.79 meters, which, although slightly thicker than Portland concrete, provided superior neutron attenuation. More notably, the thickness requirements for other sections, such as the left labyrinth (0.35 meters) and the outer labyrinth (0.1 meters), were significantly reduced compared to Portland concrete. This efficiency is attributed to boron's ability to capture neutrons effectively, thereby minimizing the scattering and subsequent radiation leakage.

Despite these advantages, the high cost and limited availability of boron poses significant challenges for large-scale implementation, especially in regions like Indonesia where resource constraints may limit the feasibility of using boron concrete extensively. Additionally, the incorporation of boron may affect the mechanical properties of the concrete, necessitating further studies to balance shielding performance with structural integrity.

Barite concrete emerged as the most effective material among the three evaluated types, primarily due to its superior density and high atomic number. Barite significantly enhances photon attenuation, making barite concrete exceptionally effective for gamma radiation shielding. The optimized design required a front shielding thickness of only 0.56 meters, substantially thinner than both Portland and boron concretes, while still maintaining radiation levels well within safety thresholds. This is relevan with the study from Awadeen *et al.* (2023) [35] reporting that barite concretes enhance the linear attenuation coefficient.

The high density of barite concrete contributes to a higher attenuation coefficient, although the exact value was not explicitly calculated in this study. The dense atomic structure facilitates greater interaction with gamma photons, thereby enhancing the concrete's ability to absorb and scatter radiation effectively. Furthermore, barite's high atomic number results in increased photoelectric absorption and Compton scattering, which are critical mechanisms in gamma attenuation.

However, the increased density of barite concrete may lead to higher material costs and logistical challenges in transportation and handling. Additionally, the high mass of barite concrete may impose additional structural requirements on the shielding design, necessitating careful consideration of the overall building design to accommodate the increased load.

Portland concrete remains the most feasible option due to its widespread availability, compliance with the SNI, and lower cost. However, its requirement for greater thickness to achieve adequate gamma shielding may lead to increased construction costs and spatial constraints, particularly in facilities where space is at a premium.

Boron concrete offers enhanced neutron attenuation with reduced thickness requirements, making it suitable for specialized applications where neutron radiation is a primary concern. Nonetheless, the high cost and limited availability of boron materials limit its practicality for widespread use, especially in resource-constrained settings.

Barite concrete presents an optimal solution for environments requiring robust gamma shielding with minimal thickness. Its superior density and atomic composition make it highly effective for photon attenuation, allowing for thinner shielding walls and potentially reducing material costs in the long run despite the higher initial expense. However, the logistical challenges associated with handling and transporting dense materials like barite concrete must be addressed to facilitate its adoption in large-scale projects.

The iterative design process was employed in optimizing the shielding configurations for each concrete type. The design was progressively refined to meet the stringent safety standards set by regulatory bodies. This methodical approach ensured that the final designs were both effective and efficient, balancing material usage with shielding performance.

One critical consideration during the design process was the presence of doors within the labyrinth structure. Doors inherently act as weak points in the shielding configuration, as they

[DOI: 10.61186/ijrr.23.4.15]

introduce gaps that can potentially allow radiation leakage. To mitigate this risk, the design incorporated dual-door systems and additional materials, such as boron stainless steel, to reduce the likelihood of neutron penetration. However, these measures also limited the extent to which the labyrinth could be optimized around doorways without compromising accessibility.

Another significant factor influencing the design was the skyshine effect, which involves the scattering of radiation upward and its subsequent downward diffusion. This phenomenon necessitated thicker shielding on the top layers to account for the increased radiation exposure resulting from upward-directed radiation. Consequently, the Y-axis shielding required careful calibration to ensure adequate protection while minimizing material usage.

Furthermore, the importance of considering both primary and secondary shielding layers. Primary shielding, located closest to the radiation source, must be sufficiently thick to attenuate the majority of the radiation. Secondary shielding, positioned further away, benefits from the attenuation already achieved by the primary layer, allowing for thinner walls without compromising overall protection. This layered approach enhances the overall shielding effectiveness while optimizing material usage.

The results of this research are consistent with previous studies indicating that high-density concretes, particularly those incorporating barite, offer superior photon attenuation. Zhou *et al*. (2023) [34] and Awadeen *et al*. (2023) [35] report that barite concretes enhance the linear attenuation coefficient by up to 13-18% and 20%, respectively, compared to ordinary concretes. Likewise, Barbhuiya *et al*. (2024) [36] emphasize the importance of composition, density, and thickness in optimizing shielding performance, while Al-Saleh *et al*. (2023) [37] demonstrate the potential of advanced composites containing heavy metal oxide nanoparticles. Collectively, these studies confirm that barite concretes remain highly effective and practical for gamma radiation shielding.

In the context of BNCT facilities, variations in thickness and dose rates are closely tied to unique room dimensions, BSA geometries, and material choices. Magni *et al*. (2020) [38] and Lai *et al*. (2020) [39] highlight that tailored designs, accurate modeling, and hybrid deterministic/Monte Carlo simulations are crucial for effective shielding. Luo (2023) [40] further shows that optimizing the BSA configuration can significantly improve neutron flux while reducing facility volume, thereby affecting overall shielding requirements. Similarly, Lee *et al*. (2021) [41] illustrate how different BSA designs influence neutron beam quality and intensity, underlining the need for facility-specific solutions that address discrepancies in dose distribution.

Comparative analyses of different concretes-such as Portland, boron-loaded, and barite-enriched-offer additional insights. Studies by Martellucci *et al*. (2021) [42], Sato *et al.* (2018) [43], and Çelen *et al.* (2019) [44] and Mansouri *et al.* (2020) [45] indicate that material properties, neutron cross-section profiles, and environmental adaptability play crucial roles in selecting suitable shielding solutions. Barite concrete, with its high density and effective attenuation characteristics, balances performance with practical considerations, while boron-loaded concretes specifically target neutron reduction. These findings collectively support more informed, context-dependent decisions in choosing and designing radiation shielding materials for cyclotron chambers and related facilities. Regarding limitation of the study, it primarily relies on simulation data to evaluate the shielding performance of different material types. The simulations offer valuable insights and allow for thorough analysis under controlled conditions.

CONCLUSION

This study highlights the comparative effectiveness of Portland, boron, and barite concretes for radiation shielding in BNCT facilities. Portland concrete, although cost-effective and widely available, requires greater thickness for adequate attenuation. Boron and barite concretes offer superior shielding at reduced thicknesses due to boron's neutron absorption and barite's high density. However, higher costs and limited availability of boron and barite concretes are challenges, especially in resource-constrained settings like Indonesia. A hybrid approach, combining Portland concrete with targeted applications of boron or barite concrete, is recommended to balance cost and performance. Future research should focus on experimental validation and cost-effective hybrid materials development.

***Acknowledgment*:** The JAEA utilized the official PHITS license. We greatly appreciate the assistance provided by the JAEA in supporting the simulation process. Additionally, we acknowledge the use of AI-based tools, including OpenAI's language model, for facilitating manuscript preparation, including drafting, editing, and improving the quality of the document.

***Conflicts of interests*:** The authors declare that they have no conflicts of interest.

***Ethical consideration*:** This research focuses solely on computational modeling and simulations, excluding any use of human or animal subjects. Consequently, no direct human or animal data were gathered. The primary software employed in this study is PHITS, which is licensed from the Japan Atomic Energy Agency (JAEA).

***Funding*:** This research did not receive any support

[DOI: 10.61186/ijrr.23.4.15]

from governmental, private, or non-profit sector funding bodies.

***Author contribution*:** A.R.W.W.: Simulation design, data analysis, and manuscript drafting; A.M.: Data curation, simulation validation, and critical manuscript review; Y.S., G.S.W., I.M.T.: Study conceptualization, project supervision, and manuscript revision; Z.I., S.U.: Project supervision, methodology refinement, and final manuscript review; H.P., N.N., N.R.H., F.: Material selection, experimental setup, and data validation; Y.K.: Technical expertise, data interpretation, and manuscript review.

REFERENCES

1. Frick C, Rumgay H, Vignat J, Ginsburg O, Nolte E, Bray F, *et al.* (2023) Quantitative estimates of preventable and treatable deaths from 36 cancers worldwide: a population-based study. *Lancet Glob Health,* ***11****(11): e1700-12.* Available from: https://doi.org/10.1016/S2214-109X(23)00406-0
2. Sung H, Ferlay J, Siegel RL, Laversanne M, Soerjomataram I, Jemal A, *et al.* (2021) Global cancer statistics 2020: globocan estimates of incidence and mortality worldwide for 36 cancers in 185 countries. *CA Cancer J Clin,* ***71****(3): 209-49.*
3. Vanita Sharma Stewart H Kerr ZK, Kerr DJ (2011) Challenges of cancer control in developing countries: current status and future perspective. *Future Oncology,* ***7****(10): 1213-22.* https://doi.org/10.2217/fon.11.101
4. Yao N, Wang J, Cai Y, Yuan J, Wang H, Gong J, *et al.* (2016) Patterns of cancer screening, incidence and treatment disparities in China: protocol for a population-based study. *BMJ Open,* ***6****(8): e012028.* http://bmjopen.bmj.com/content/6/8/e012028.abstract
5. Feliciano EJG, Ho FD V, Yee K, Paguio JA, Eala MAB, Robredo JPG, *et al.* (2023) Cancer disparities in Southeast Asia: intersectionality and a call to action. *Lancet Reg Health West Pac,* ***41****: 100971.* https://doi.org/10.1016/j.lanwpc.2023.100971
6. Minas TZ, Kiely M, Ajao A, Ambs S (2021) An overview of cancer health disparities: new approaches and insights and why they matter. *Carcinogenesis,* ***42****(1): 2-13.* https://doi.org/10.1093/carcin/bgaa121
7. Li L, Shan T, Zhang D, Ma F (2024) Nowcasting and forecasting global aging and cancer burden: analysis of data from the GLOBOCAN and Global Burden of Disease Study. *Journal of the National Cancer Center,* ***4****(3):223-32.* https://www.sciencedirect.com/science/article/pii/S2667005424000280
8. Are C (2023) JSO seminar series: Global inequities in access to cancer care and strategies to address them. *J Surg Oncol,* ***128****(6): 929-30.* https://doi.org/10.1002/jso.27476
9. Thun MJ, DeLancey JO, Center MM, Jemal A, Ward EM (2010) The global burden of cancer: priorities for prevention. *Carcinogenesis,* ***31****(1): 100-10.* https://doi.org/10.1093/carcin/bgp263
10. Sha R, Kong X meng, Li X yu, Wang Y bing (2024) Global burden of breast cancer and attributable risk factors in 204 countries and territories, from 1990 to 2021: results from the Global Burden of Disease Study 2021. *Biomark Res,* ***12****(1): 87.* https://doi.org/10.1186/s40364-024-00631-8
11. Lertkhachonsuk A aroon, Yip CH, Khuhaprema T, Chen DS, Plummer M, Jee SH, *et al.* (2013) Cancer prevention in Asia: resource-stratified guidelines from the Asian Oncology Summit 2013. *Lancet Oncol,* ***14****(12): e497-507.* https://doi.org/10.1016/S1470-2045(13)70350-4
12. Onyoh EF, Hsu WF, Chang LC, Lee YC, Wu MS, Chiu HM (2019) The rise of colorectal cancer in Asia: Epidemiology, screening, and management. *Curr Gastroenterol Rep,* ***21****(8): 36.* https://doi.org/10.1007/s11894-019-0703-8
13. Varmus H and Kumar HS (2013) Addressing the growing international challenge of cancer: A multinational perspective. *Sci Transl Med,* ***5****(175): 175cm2.* https://doi.org/10.1126/scitranslmed.3005899
14. He H, Li J, Jiang P, Tian S, Wang H, Fan R, *et al.* (2021) The basis and advances in clinical application of boron neutron capture therapy. *Radiation Oncology,* ***16****(1): 216.* https://doi.org/10.1186/s13014-021-01939-7
15. Bortolussi S, Liu YH, Porras I (2021) Boron neutron capture therapy: From nuclear physics to biomedicine. *Biology (Basel),* ***10****(5): 370.* https://www.mdpi.com/2079-7737/10/5/370
16. Miyatake SI, Kawabata S, Hiramitsu R, Kuroiwa T, Suzuki M, Kondo N, *et al.* (2016) Boron neutron capture therapy for malignant brain tumors. *Neurol Med Chir (Tokyo),* ***56****(7): 361-71.*
17. Hatanaka H, Amano K, Kamano Sh, Fankhauser H, Hanamura T, Sano K (1978) Boron-neutron capture therapy in relation to immunotherapy. *Acta Neurochir (Wien),* ***42****(1): 57-72.* https://doi.org/10.1007/BF01406631
18. Lan TL, Lin CF, Lee YY, Lin KH, Chang FC, Lin SC, *et al.* (2023) Advances in boron neutron capture therapy (BNCT) for recurrent intracranial meningioma. *Int J Mol Sci,* ***24****(5): 4978.* https://www.mdpi.com/1422-0067/24/5/4978
19. Barth RF, Gupta N, Kawabata S (2024) Evaluation of sodium borocaptate (BSH) and boronophenylalanine (BPA) as boron delivery agents for neutron capture therapy (NCT) of cancer: an update and a guide for the future clinical evaluation of new boron delivery agents for NCT. *Cancer Commun,* ***44****(8): 893-909.* https://doi.org/10.1002/cac2.12582
20. Skwierawska D, López-Valverde JA, Balcerzyk M, Leal A (2022) Clinical viability of boron neutron capture therapy for personalized radiation treatment. *Cancers (Basel),* ***14****(12): 2865.* https://www.mdpi.com/2072-6694/14/12/2865
21. Seneviratne D, Advani P, Trifiletti DM, Chumsri S, Beltran CJ, Bush AF, *et al.* (2022) Exploring the biological and physical basis of boron neutron capture therapy (BNCT) as a promising treatment frontier in breast cancer. *Cancers (Basel),* ***14****(12): 3009.* https://www.mdpi.com/2072-6694/14/12/3009
22. Dymova MA, Taskaev SY, Richter VA, Kuligina EV (2020)Boron neutron capture therapy: Current status and future perspectives. *Cancer Commun,* ***40****(9): 406-21.* https://doi.org/10.1002/cac2.12089
23. Tsoulfanidis N (2010) Measurement and detection of radiation. 3rd ed. CRC Press.
24. BAPETEN. Perka Bapeten No 4 Tahun 2013 tentang Proteksi dan Keselamatan Radiasi dalam Pemanfaatan Tenaga Nuklir [Internet]. 2013. https://www.bapeten.go.id/
25. Oudiz A, Croft J, Fleishman A, Lochardj Lombard J, Webb G (1986) What is ALARA ? IAEA Press.
26. Priambodo G, Nugroho F, Palupi DS, Zailani R, Sardjono Y (2017) Optimasi perisai radiasi neutron fasilitas ruangan iradiasi untuk boron neutron capture cancer therapy (BNCT) dengan sumber beamport tembus reaktor kartini. *Jurnal Teknologi Reaktor Nuklir Tri Dasa Mega,* ***19****(3): 139-46.*
27. Mu'Alim M and Sardjono Y (2018) Modeling the radiation shielding of boron neutron capture therapy based on 2.4 MeV D-D neutron generator facility. *Jurnal Teknologi Reaktor Nuklir Tri Dasa Mega,* ***20****(1): 1-8.*
28. Sato T, Shtotfs YI Atkpetnmhinsls I, Niita K (2018) Features of Particle and heavy ion transport code system (PHITS) version 3.02. *J Nucl Sci Technol,* ***55****(6): 684-90.* https://doi.org/10.1080/00223131.2017.1419890
29. Nemati MJ, Habibi M, Amrollahi R (2013) Analysis of concrete labyrinth shielding and radiation dose for APF plasma focus neutron source by FLUKA Monte Carlo code. *J Radioanal Nucl Chem,* ***295****(1): 221-6.* https://doi.org/10.1007/s10967-012-2196-x
30. Kashiwagi H, Kawabata S, Yoshimura K, Fukuo Y, Kanemitsu T, Takeuchi K, *et al.* (2022) Boron neutron capture therapy using dodecaborated albumin conjugates with maleimide is effective in a rat glioma model. *Invest New Drugs,* ***40****(2): 255-64.* https://doi.org/10.1007/s10637-021-01201-7
31. Oloo SO, Smith KM, Vicente M da GH (2023) Multi-functional boron -delivery agents for boron neutron capture therapy of cancers. *Cancers,* ***15****(13): 3277.* https://www.mdpi.com/2072-6694/15/13/3277
32. McConn RJ, Gesh CJ, Pagh RT, Rucker RA (2011) Radiation portal monitor project compendium of material composition data for radiation transport modeling. PIET-43741-TM-963 PNNL-15870 Rev. 1, Technical report.
33. Ardana IM and Sardjono Y (2017) Optimization of a neutron beam shaping assembly design for BNCT and its dosimetry simulation based on MCNPX. *Jurnal Teknologi Reaktor Nuklir Tri Dasa Mega,* ***19****(3): 121.*
34. Zhou Y, Chen X, Zhan Y, Sun F, Zhang J, He W (2023) Research on the shielding performance of concrete in a 60Co irradiation environment. *Nuclear Engineering and Design,* ***413****: 112575.* https://www.sciencedirect.com/science/article/pii/

[DOI: 10.61186/ijrr.23.4.15]

S0029549323004247
35. Awadeen M, Amin M, Bakr RH, Tahwia AM (2024) Mechanical properties, attenuation coefficient, and microstructure of ultra high-performance heavyweight concrete for radiation shielding applications. *Journal of Building Engineering,* ***82****: 108395*. https://www.sciencedirect.com/science/article/pii/S2352710223025780
36. Barbhuiya S, Das BB, Norman P, Qureshi T (2024) A comprehensive review of radiation shielding concrete: Properties, design, evaluation, and applications. *Structural Concrete,* ***26****(2): 1809-1855*. Available from: https://doi.org/10.1002/suco.202400519
37. Al-Saleh WM, Almutairi HM, Sayyed MI, Elsafi M (2023) Multilayer radiation shielding system with advanced composites containing heavy metal oxide nanoparticles: a free-lead solution. *Sci Rep,* ***13****(1): 18429*. https://doi.org/10.1038/s41598-023-45621-2
38. Magni C, Postuma I, Ferrarini M, Protti N, Fatemi S, Gong C, *et al*. (2020) Design of a BNCT irradiation room based on proton accelerator and beryllium target. *Applied Radiation and Isotopes,* ***165****: 109314*. https://www.sciencedirect.com/science/article/pii/S0969804320304644
39. Lai BL, Huang YS, Lai PC, Chu WH, Sheu RJ (2020) Comparison of different methods for the shielding analysis of an AB-BNCT facility based on the Be(p,xn) reaction with 30-MeV protons. *Applied Radiation and Isotopes,* ***166****: 109351.* https://www.sciencedirect.com/science/article/pii/S0969804320304991
40. Luo Y, Seidl M, Wang X (2023) Design and verification of BNCT beam shaping assembly based on genetic algorithm. In: Liu C, editor. Proceedings of the 23rd Pacific Basin Nuclear Conference, Volume 2. Singapore: Springer Nature Singapore;. p. 306-15.
41. Lee PY, Tang X, Geng C, Liu YH (2021) A bi-tapered and air-gapped beam shaping assembly used for AB-BNCT. *Applied Radiation and Isotopes,* ***167****: 109392*. https://www.sciencedirect.com/science/article/pii/S096980432030539X
42. Martellucci M, Romanelli G, Valeri S, Cottone D, Andreani C, Senesi R (2021) The neutron cross section of barite-enriched concrete for radioprotection shielding in the range 1 meV–1 keV. *The European Physical Journal Plus,* ***136****(2): 259*. https://doi.org/10.1140/epjp/s13360-021-01243-z
43. Sato S, Konno C, Nakashima H, Shionaga R, Nose H, Ito Y, *et al*. (2018) Shielding performance of newly developed boron-loaded concrete for DT neutrons. *J Nucl Sci Technol,* ***55****(4): 410-7.* https://doi.org/10.1080/00223131.2017.1403380
44. Çelen YY, Evcin A, Akkurt I, Bezir NÇ, Günoğlu K, Kutu N (2019) Evaluation of boron waste and barite against radiation. *International Journal of Environmental Science and Technology,* ***16****(9): 5267-74*. https://doi.org/10.1007/s13762-019-02333-3
45. Mansouri E, Mesbahi A, Malekzadeh R, Ghasemi Janghjoo A, Okutan M (2020) A review on neutron shielding performance of nanocomposite materials. *International Journal of Radiation Research,* ***18****(4): 611-22.*

[DOI: 10.61186/ijrr.23.4.15]